Theory of frequency shifts in the oscillating cantilever-driven adiabatic reversals technique as a function of the spin location

G. P. Berman,[1] F. Borgonovi,[2,3] and V. I. Tsifrinovich[4]
[1]*Theoretical Division and CNLS, MS B213, Los Alamos National Laboratory, Los Alamos, New Mexico 87545, USA*
[2]*Dipartimento di Matematica e Fisica, Universitá Cattolica, via Musei 41, 25121 Brescia, Italy*
[3]*INFN, Sezione di Pavia, Italy*
[4]*IDS Department, Polytechnic University, Six Metrotech Center, Brooklyn, New York 11201, USA*
(Received 9 May 2005; revised manuscript received 29 August 2005; published 6 December 2005)

The theory of the oscillating cantilever-driven adiabatic reversals (OSCAR) in magnetic resonance force microscopy (MRFM) is extended to describe the relation between an external magnetic field and a dipole magnetic field for an arbitrary location of the single spin. An analytical estimate for the OSCAR MRFM frequency shift is derived and shown to be in excellent agreement with numerical simulations. The dependence of the frequency shift on the position of the spin relative to the cantilever has characteristic maxima and minima which can be used to determine the spin location experimentally.

DOI: 10.1103/PhysRevB.72.224406 PACS number(s): 76.60.−k, 07.55.−w

I. INTRODUCTION

Magnetic resonance force microscopy (MRFM) has attracted much attention as a promising way to the magnetic resonance imagine with the atomic scale resolution.[1–3] In particular, the oscillating cantilever-driven adiabatic reversals (OSCAR) technique in MRFM introduced in Ref. 4 has been used to successfully detect a single electron spin below the surface of a solid.[5] In the OSCAR MRFM technique the vibrations of the cantilever tip (CT) with an attached ferromagnetic particle in the presence of a rf magnetic field cause the periodic reversals of the effective magnetic field acting on the single electron spin. If the conditions of adiabatic motion are satisfied the spin follows the effective magnetic field. The back action of the spin on the CT causes a small frequency shift of the CT vibrations, which can be measured with high precision.

The quasiclassical theory of OSCAR MRFM has been developed in Ref. 6. This theory contains two important limitations. First, it assumes that the external magnetic field $\vec{B}_{ext}$ at the spin is much greater than the dipole field $\vec{B}_d$ produced by the ferromagnetic particle. In real experiments, in order to increase the frequency shift $\delta\omega_c$, one has to decrease the distance between the CT and the spin to values where the dipole field becomes sometimes greater than the external field.[5] Second, it was assumed in Ref. 6 that the spin is located in the plane of the cantilever vibrations. Thus the quasiclassical theory should be extended in order to describe both an arbitrary relation between $\vec{B}_{ext}$ and $\vec{B}_d$ and an arbitrary location of the spin. This extension is presented in our paper.

A single spin is a quantum object which must be described using quantum theory. The quantum theory of OSCAR MRFM has been developed in Ref. 7 with the same limitations as the quasiclassical theory. It was found, as may be expected, that the frequency shift $\delta\omega_c$ in quantum theory may assume only two values $\pm|\delta\omega_c|$ corresponding to the two directions of the spin relative to the effective magnetic field. The value of $|\delta\omega_c|$ in quantum theory is the same as the maximum frequency shift calculated using quasiclassical theory (where it can take any value between $-|\delta\omega_c|$ and $|\delta\omega_c|$). Thus, to calculate the quantum frequency shift, it is reasonable to use quasiclassical instead of quantum theory.

II. EQUATIONS OF MOTION

We consider the MRFM setup shown in Fig. 1. The CT oscillates in the *x*-*z* plane. The origin is placed at the equilibrium position of the center of the ferromagnetic particle. Note that here we ignore the static displacement of the CT caused by the magnetic force of the spin. The magnetic moment of the spin, $\vec{\mu}$ shown in Fig. 1, points initially in the direction of the magnetic field $\vec{B}_0$, which corresponds to the equilibrium position of CT [see Eq. (4)]. We assume now that the rf magnetic field $2\vec{B}_1$ is linearly polarized in the plane which is perpendicular to $\vec{B}_0$. (Later we will generalize

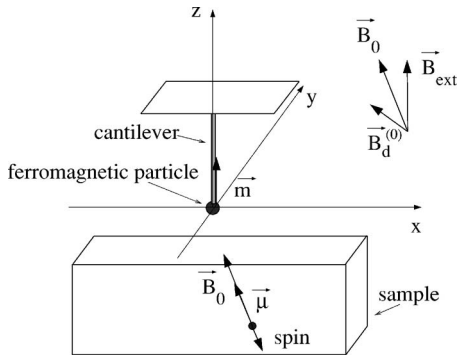

FIG. 1. MRFM setup. The equilibrium position of the spin and the cantilever with a spherical ferromagnetic particle. $\vec{m}$ is the magnetic moment of the ferromagnetic particle, $\vec{\mu}$ is the magnetic moment of the spin, $\vec{B}_{ext}$, $\vec{B}_d^{(0)}$, and $\vec{B}_0$ are, respectively, the external permanent magnetic field, the dipole field on the spin, and the net magnetic field. In general the vectors $\vec{B}_d^{(0)}$ and $\vec{B}_0$ do not lie in the *x*-*z* plane.

this to an arbitrary direction of polarization.) The dipole magnetic field $\vec{B}_d$ is given by:

$$\vec{B}_d = \frac{\mu_0}{4\pi}\frac{3(\vec{m}\cdot\vec{n})\vec{n}-\vec{m}}{r_v^3}, \tag{1}$$

where $\vec{m}$ is the magnetic moment of the ferromagnetic particle pointing in the positive z-direction, r_v is the (variable) distance between the moving CT and the stationary spin, and $\vec{n}$ is the unit vector pointing from the CT to the spin. We define:

$$r_v = \sqrt{(x-x_c)^2+y^2+z^2}, \tag{2}$$

$$\vec{n} = \left(\frac{x-x_c}{r_v}, \frac{y}{r_v}, \frac{z}{r_v}\right), \tag{3}$$

where x, y, z are the spin coordinates, and x_c is the CT coordinate (i.e., the coordinate of the center of the ferromagnetic particle). At the equilibrium, the net magnetic field at the spin is

$$\vec{B}_0 = \vec{B}_{ext} + \vec{B}_d^{(0)}, \tag{4}$$

$$\vec{B}_d^{(0)} = \frac{3m\mu_0}{4\pi r^5}\left(zx, zy, z^2 - \frac{r^2}{3}\right), \tag{5}$$

$$\vec{B}_{ext} = (0,0,B_{ext}), \tag{6}$$

where $r=\sqrt{x^2+y^2+z^2}$. In the approximation which is linear in x_c, the magnetic field $\vec{B}_d$ changes by the value of $\vec{B}_d^{(1)}$:

$$\vec{B}_d^{(1)} = -(G_x, G_y, G_z)x_c, \tag{7}$$

$$(G_x, G_y, G_z) = \frac{3m\mu_0}{4\pi r^7}(z(r^2-5x^2), -5xyz, x(r^2-5z^2)), \tag{8}$$

where (G_x, G_y, G_z) describes the gradient of the magnetic field at the spin location at $x_c=0$:

$$(G_x, G_y, G_z) = \left(\frac{\partial B_d^x}{\partial x}, \frac{\partial B_d^y}{\partial x}, \frac{\partial B_d^z}{\partial x}\right). \tag{9}$$

(Note that the magnetic field and its gradient depend on the CT coordinate x_c.) Next we consider the equation of motion for the spin magnetic moment $\vec{\mu}$ in the system of coordinates rotating with the rf field at frequency ω about the magnetic field $\vec{B}_0$. (The $\tilde{z}$ axis of this new system points in the direction of $\vec{B}_0$.) We have

$$\dot{\vec{\mu}} = -\gamma\vec{\mu}\times\vec{B}_{eff},$$

$$\vec{B}_{eff} = [B_1, 0, B_0 - (\omega/\gamma) - x_c\sum_i G_i\cos\alpha_i],$$

$$\cos\alpha_i = B_0^i/B_0. \tag{10}$$

Here α_i $(i=x,y,z)$ are the angles between the direction of the magnetic field $\vec{B}_0$ and the axes x, y, z of the laboratory system of coordinates; and γ is the gyromagnetic ratio of the electron spin. (γ is the absolute value of the gyromagnetic ratio.) We ignore the transverse components of the dipole field $\vec{B}_d$ because they represent the fast oscillating terms in the rotating system of coordinate. Also we consider only the rotating component of the rf magnetic field.

The equations of motion for the CT can be written as

$$\ddot{x}_c + \omega_c^2 x_c = F_x/m^*, \tag{11}$$

where ω_c and m^* are the frequency and the effective mass of the CT and F_x is the magnetic force acting on the ferromagnetic particle on CT. We consider the CT oscillations in the laboratory system of coordinates. Ignoring fast oscillating terms in the laboratory system, we obtain

$$F_x = -\mu_{\tilde{z}}\sum_i G_i\cos\alpha_i. \tag{12}$$

Next, we will use the following units: for time $1/\omega_c$, for magnetic moment μ_B, for magnetic field ω_c/γ, for length the characteristic distance L_0 between CT and the spin, and for force k_cL_0, where $k_c=m^*\omega_c^2$ is the effective CT spring constant. Using these units, we derive the following dimensionless equations of motion:

$$\dot{\vec{\mu}} = -\vec{\mu}\times\vec{B}_{eff},$$

$$\ddot{x}_c + x_c = F_x,$$

$$\vec{B}_{eff} = (B_1, 0, \Delta - \beta\mathcal{G}x_c),$$

$$F_x = -\alpha\beta\mathcal{G}\mu_{\tilde{z}},$$

$$\Delta = B_0 - \omega,$$

$$\mathcal{G} = \frac{1}{r^7}[z(r^2-5x^2)\cos\alpha_x - 5xyz\cos\alpha_y + x(r^2-5z^2)\cos\alpha_z]. \tag{13}$$

The parameters α and β are given by

$$\alpha = \frac{\mu_B\omega_c}{\gamma k_c L_0^2}, \quad \beta = \frac{3\gamma\mu_0 m}{4\pi\omega_c L_0^3}. \tag{14}$$

Note that all quantities in Eq. (13) are dimensionless, i.e., x means x/L_0, μ means μ/μ_B, B_0 means $\gamma B_0/\omega_c$, and so on. In terms of dimensional quantities the parameter β is the ratio of the dipole frequency $\gamma B_d^{(0)}$ to the CT frequency ω_c, and the product $\alpha\beta$ is the ratio of the static CT displacement F_x/k_c to the CT-spin distance L_0. The derived equations are convenient for both numerical simulations and analytical estimates.

III. THE OSCAR MRFM FREQUENCY SHIFT

In this section we present the analytical estimates and the numerical simulations for the OSCAR MRFM frequency shift. When the CT oscillates, the resonant condition ω

$=\gamma|\vec{B}_{ext}+\vec{B}_d|$ can be satisfied only if the spin is located inside the resonant slice which is defined by its boundaries:

$$|\vec{B}_{ext}+\vec{B}_d(x_c=\pm A)|=\omega/\gamma, \tag{15}$$

where A is the amplitude of the CT vibrations. For an analytical estimate, we assume that the spin is located at the central surface of the resonant slice. In this case in Eq. (13) $\Delta=0$.

To obtain an analytical estimate for the OSCAR MRFM frequency shift we will assume an ideal adiabatic motion and put $\dot{\vec{\mu}}=0$ in Eq. (13). Let the CT begin its motion (at $t=0$) from the right end position $x_c(0)=A$. Then the initial direction (i.e., at $t=0$) of the effective magnetic field $\vec{B}_{eff}$ relative to the magnetic field $\vec{B}_{ext}+\vec{B}_d$ and of the magnetic moment $\vec{\mu}$ depends on the sign of $\mathcal{G}$: $\vec{B}_{eff}$ and $\vec{\mu}$ have the same direction for $\mathcal{G}<0$ and opposite directions for $\mathcal{G}>0$. Substituting the derived expression for $\mu_{\tilde{z}}\simeq -B^z_{eff}\mathcal{G}/|\vec{B}_{eff}||\mathcal{G}|$ into F_x we obtain the following equation for x_c:

$$\ddot{x}_c+x_c\left\{1+\frac{\alpha\beta^2\mathcal{G}|\mathcal{G}|}{\sqrt{B_1^2+(\beta\mathcal{G}x_c)^2}}\right\}=0. \tag{16}$$

We solve this equation as in Ref. 6, using the perturbation theory of Bogoliubov and Mitropolsky,[8] and we find the dimensionless frequency shift (see the Appendix):

$$\delta\omega_c\simeq\frac{2}{\pi}\frac{\alpha\beta^2\mathcal{G}|\mathcal{G}|}{\sqrt{B_1^2+(\beta\mathcal{G}A)^2}}\left\{1+\frac{1}{2}\frac{B_1^2}{B_1^2+(\beta\mathcal{G}A)^2}\times\left[\ln\left(\frac{4\sqrt{B_1^2+(\beta\mathcal{G}A)^2}}{B_1}\right)+\frac{1}{2}\right]\right\}. \tag{17}$$

In typical experimental conditions we have

$$B_1\ll\beta\mathcal{G}A,$$

and Eq. (17) transforms to the simple expression

$$\delta\omega_c=\frac{2}{\pi}\frac{\alpha\beta\mathcal{G}}{A}. \tag{18}$$

One can see that the frequency shift is determined by the ratio of the static CT displacement F_x/k_c to the amplitude of the CT vibrations A. We will also present Eq. (17) in terms of dimensionless quantities:

$$\frac{\delta\omega_c}{\omega_c}=\frac{2\mu_B G_0}{\pi A k_c}, \tag{19}$$

where

$$G_0=\sum_i G_i\cos\alpha_i. \tag{20}$$

Equations (17) and (19) represent an extension of the estimate derived in Ref. 6. These equations are valid for any point on the central resonant surface and for any relation between $\vec{B}_{ext}$ and $\vec{B}_d$. It follows from Eq. (17) that $\delta\omega_c$ is an even function of y and an odd function of x.

In our computer simulations we have used the following parameters taken from experiments:[5]

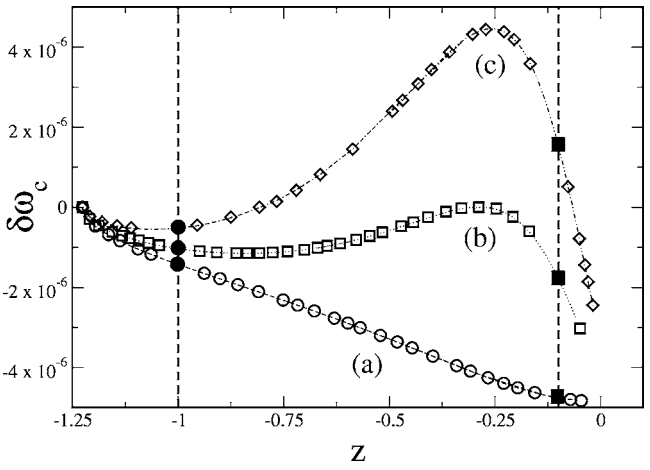

FIG. 2. The OSCAR MRFM frequency shift $\delta\omega_c(z)$ at the central resonant surface ($\Delta=0$), for $x>0$. The symbols show the numerical data, the lines correspond to the estimate (17) for (a) $y=0$ (circles), (b) $y=x/2$ (squares), and (c) $y=x$ (diamonds). Solid squares and circles indicate frequency shifts at the spin locations indicated in Fig. 3. In all figures the coordinates x, y, and z are in units of L_0 and the frequencies are in units of ω_c.

$$\omega/2\pi=5.5\text{ kHz},\quad k_c=110\ \mu\text{N/m},\quad A=16\text{ nm},$$

$$B_{ext}=30\text{ mT},\quad \omega/2\pi=2.96\text{ GHz},\quad \omega/\gamma=106\text{ mT},$$

$$|G_z|=2\times10^5\text{ T/m},\quad B_1=300\ \mu\text{T},\quad L_0\approx350\text{ nm}.$$

The corresponding dimensionless parameters are the following:

$$\alpha=1.35\times10^{-13},\quad \beta=1.07\times10^6,\quad A=4.6\times10^{-2},$$

$$B_1=1.5\times10^3,\quad B_{ext}=1.53\times10^5,\quad \omega=5.4\times10^5.$$

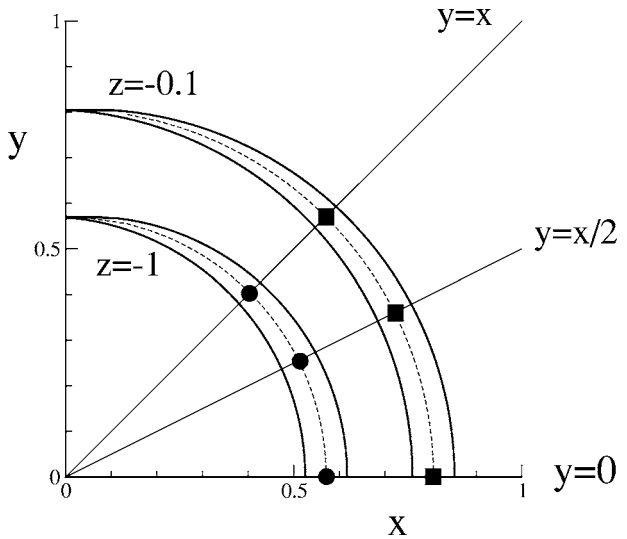

FIG. 3. Cross sections of the resonant slice for $z=-0.1$ and $z=-1$. The dashed lines show the intersection between the cross sections and the central resonant surface. The solid squares and circles indicate spin locations which correspond to the frequency shifts given by the same symbols in Fig. 2.

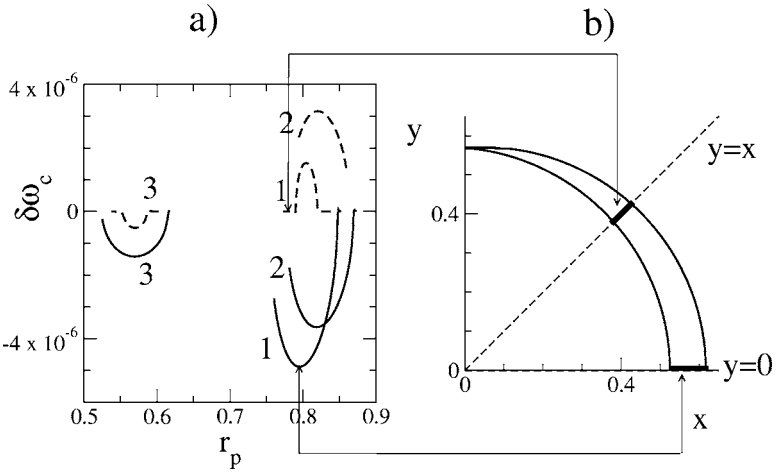

FIG. 4. (a) The OSCAR MRFM frequency shift $\delta\omega_c(r_p)$ inside the cross-sectional area of the resonant slice for $x>0$. The solid lines correspond to $y=0$ and the dashed lines correspond to $y=x$. Lines are 1, $z=-0.1$,2, $z=-0.43$, and 3, $z=-1$. $r_p=(x^2+y^2)^{1/2}$. (b) The cross section of the resonant slice $z=-0.1$. The bold segments show the spin locations which correspond to lines 1 in (a).

As initial conditions we take

$$\vec{\mu}(0)=(0,0,1), \quad x_c(0)=A, \quad \dot{x}_c(0)=0.$$

Below we describe the results of our computer simulations. Figure 2 shows the frequency shift $\delta\omega_c$ as a function of the spin z-coordinate at the central resonant surface ($\Delta=0$). First, one can see an excellent agreement between the numerical data and the analytical estimate (17). Second, as expected, the maximum magnitude of the frequency shift $|\delta\omega_c|$ can be achieved when the spin is located in the plane of the CT vibrations $y=0$. However, for $y=x$, it has almost the same magnitude $|\delta\omega_c|$ (with the opposite sign of $\delta\omega_c$). Moreover, for $y=x$ the dependence $\delta\omega_c(z)$ has an extremum, which can be used for the measurement of the spin z-coordinate. If the distance between the CT and the surface of the sample can be controlled, then the "depth" of the spin location below the sample surface can be determined. (In all figures, the coordinates x, y, and z are given in units of L_0, and the frequency shift is in units of ω_c.)

Figure 3 shows the cross sections of the resonant slice for $z=-0.1$ and $z=-1$. The greater the distance from the CT, the smaller the cross-sectional area. The solid squares and circles in Fig. 3 show the spin locations which correspond to the frequency shifts indicated by the same symbols in Fig. 2.

Figure 4 demonstrates the "radial" dependence of the frequency shift $\delta\omega_c(r_p)$, where $r_p=(x^2+y^2)^{1/2}$. The value of r_p can be changed by the lateral displacement of the cantilever. As one may expect, the maximum value of $|\delta\omega_c|$ corresponds to the central resonant surface. The maximum becomes sharper as z decreases. Thus a small distance between the CT and the sample surface is preferable for the measurement of the radial position of the spin.

Figure 5 shows the "azimuthal dependence" of the frequency shift $\delta\omega_c(\phi)$, where $\phi=\tan^{-1}(y/x)$ and the spin is located on the central resonant surface. Note that for the given values of z and ϕ, the coordinates x and y of the spin are fixed if the spin is located on the central resonant surface. The value of ϕ can be changed by rotating the cantilever about its axis. One can see the sharp extrema of the function $\delta\omega_c(\phi)$. Again, the small distance between the CT and the sample is preferable for the measurement of the "azimuthal position" of the spin.

Finally, we consider the realistic case in which the direction of polarization of the rf field $2\vec{B}_1$ is fixed in the laboratory system of coordinates. Now the angle θ between the direction of polarization of $2\vec{B}_1$ and the field $\vec{B}_0$ depends on the spin coordinate because the magnitude and the direction of the dipole field $\vec{B}_d^{(0)}$ depend on the spin location. To describe this case we ignore the component of $2\vec{B}_1$ which is parallel to $\vec{B}_0$, and change B_1 to $B_1 \sin\theta$ in all our formulas. As an example, Fig. 6 demonstrates the dependence $\delta\omega_c(z)$ for the case in which the rf field is polarized along the x axis. One can see that in a narrow region of z the magnitude of the frequency shift sharply drops. This occurs because in this region the magnetic field $\vec{B}_0$ is almost parallel to the x axis. Thus the effective field $B_1 \sin\theta$ is small: the condition of the adiabatic motion $\gamma[B_1 \sin\theta]^2 \gg |d\vec{B}_{eff}/dt|$ is not satisfied; and the spin does not follow the effective magnetic field. The dashed lines in Fig. 6 correspond to the analytical estimate

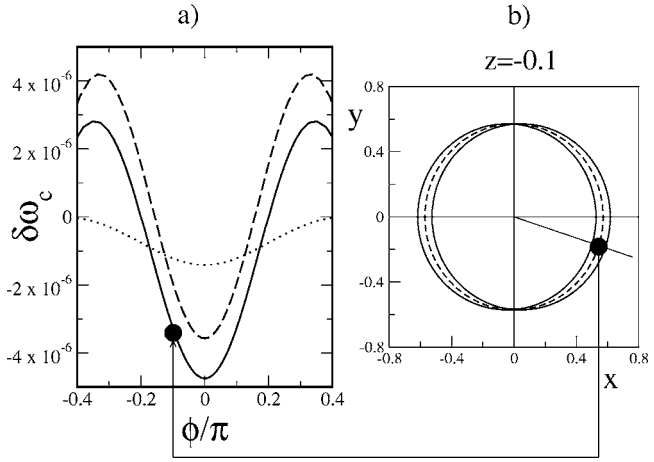

FIG. 5. (a) $\delta\omega_c(\phi)$, with $\phi=\tan^{-1}(y/x)$ for the central resonant surface: $z=-0.1$ (full line), $z=-0.43$ (dashed line), $z=-1$ (dotted line). (b) Solid line shows the cross section of the resonant slice for $z=-0.1$. Dashed line shows the intersection between the plane $z=-0.1$ and the central resonant surface. The solid circle in (b) shows the spin location $\phi/\pi=-0.1$ whose corresponding frequency shift is marked by a solid circle in (a).

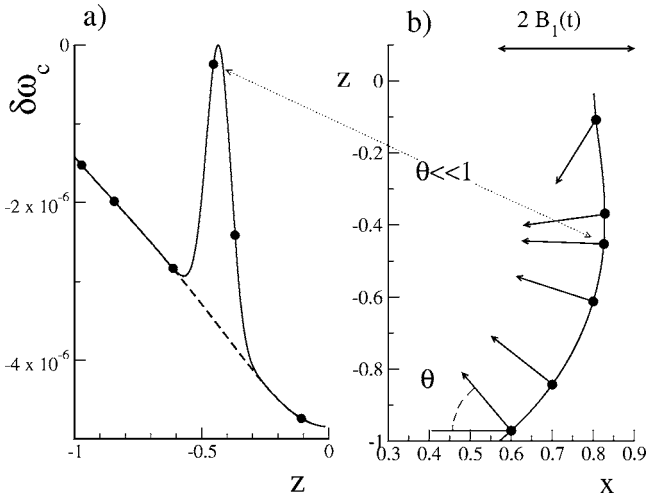

FIG. 6. (a) $\delta\omega_c(z)$ when the rf field $\vec{B}_1$ is parallel to the x axis. The spin is located at the central resonant surface $y=0$, $x>0$. Solid line is numerical data, dashed line is the analytical estimate (17), which assumes adiabatic motion of the spin magnetic moment $\vec{\mu}$ parallel to $\vec{B}_{eff}$. For a few numerical points indicated as solid cirlces in (a) the corresponding $\vec{B}_0$ field is shown in (b). (b) Solid line: intersection between the central resonant surface and the x-z plane. Arrows show the magnetic field $\vec{B}_0$ on this intersection at the points indicated as solid circles in (a). The absolute value of the frequency shift $|\delta\omega_c|$ drops at the spin locations where $\vec{B}_0$ is approximately parallel to $\vec{B}_1(\theta \ll 1)$.

(17) with the substitution $B_1 \rightarrow B_1 \sin\theta$: the analytical estimate assumes adiabatic conditions, which are violated for small θ.

The sharp drop of $|\delta\omega_c|$ could be observed either by the change of the distance between the CT and the sample surface or by the change of the direction of polarization of the rf field. In any case this effect provides an independent measurement of the spin "depth" below the sample surface.

IV. CONCLUSION

We have derived the quasiclassical equations of motion describing the OSCAR technique in MRFM for an arbitrary relation between the external and dipole magnetic fields and arbitrary location of a single spin. We have obtained an analytical estimate of the OSCAR MRFM frequency shift $\delta\omega_c$ which is in excellent agreement with numerical simulations. We have shown that the dependence $\delta\omega_c$ on the position of spin relative to the cantilever contains characteristic maxima and minima which can be used to determine the position of the spin. We believe that moving the cantilever in three dimensions, rotating it (or the sample) about the cantilever's axis, and changing the direction of the polarization of the rf magnetic field, experimentalist eventually will enable the determination of the position of a single spin. We hope that our work will help to achieve this goal.

ACKNOWLEDGMENTS

This work was supported by the Department of Energy (DOE) under Contract No. W-7405-ENG-36, by the Defense Advanced Research Projects Agency (DARPA), by the National Security Agency (NSA), and by the Advanced Research and Development Activity (ARDA).

APPENDIX

Equation (16) can be written in the following form:

$$\frac{d^2x_c}{d\tau^2} + x_c = \epsilon f(x_c), \tag{A1}$$

where $\tau=\omega_c t$ is the dimensionless time,

$$f(x_c) = \frac{\beta\mathcal{G}x_c}{\sqrt{B_1^2 + (\beta\mathcal{G})^2 x_c^2}}, \tag{A2}$$

and $\epsilon=-\alpha\beta|\mathcal{G}|$.

The approximate solution of Eq. (21) can be written as[8]

$$x_c(\tau) = a(\tau)\cos\psi(\tau) + O(\epsilon), \tag{A3}$$

where in the first order in ϵ, $a(\tau)$ and $\psi(\tau)$ satisfy the equations:

$$\frac{da}{d\tau} = \epsilon P_1(a) + O(\epsilon),$$

$$\frac{d\psi}{d\tau} = 1 + \epsilon Q_1(a) + O(\epsilon), \tag{A4}$$

and the functions $P_1(a)$ and $Q_1(a)$ are given by

$$P_1(a) = -\frac{1}{2\pi}\int_0^{2\pi} f(a\cos\psi)\sin\psi\, d\psi, \tag{A5}$$

$$Q_1(a) = -\frac{1}{2\pi a}\int_0^{2\pi} f(a\cos\psi)\cos\psi\, d\psi. \tag{A6}$$

On inserting the explicit expression (22) for $f(a\cos\psi)$ one gets:

$$P_1(a) = 0, \tag{A7}$$

$$Q_1(a) = -\frac{2\beta\mathcal{G}}{\pi\sqrt{B_1^2 + (\beta\mathcal{G}a)^2}}\int_0^{\pi/2} \frac{(1-\sin^2\psi)}{\sqrt{1-k^2\sin^2\psi}} d\psi, \tag{A8}$$

where

$$k^2 = \frac{(\beta\mathcal{G}a)^2}{B_1^2 + (\beta\mathcal{G}a)^2}. \tag{A9}$$

Equation (28) can be written as

$$Q_1(a) = -\frac{2\beta\mathcal{G}}{\pi k^2\sqrt{B_1^2 + (\beta\mathcal{G}a)^2}}[(k^2-1)K(k) + E(k)], \tag{A10}$$

where $K(k)$ and $E(k)$ are the complete elliptic integrals of the first and second kind. When $k \simeq 1$ elliptic integrals can be approximated by

$$K(k) \approx \ln \frac{4}{\sqrt{1-k^2}} + \frac{1}{4}\left(\ln \frac{4}{\sqrt{1-k^2}} - \frac{1}{2}\right)(1-k^2), \tag{A11}$$

$$E(k) \approx 1 + \frac{1}{2}\left(\ln \frac{4}{\sqrt{1-k^2}} - \frac{1}{2}\right)(1-k^2). \tag{A12}$$

In the first order approximation the frequency shift is

$$\delta\omega_c \simeq \epsilon Q_1(a) = \frac{2}{\pi}\frac{\alpha\beta^2\mathcal{G}|\mathcal{G}|}{\sqrt{B_1^2+(\beta\mathcal{G}a)^2}}\left\{1+\frac{1}{2}\frac{B_1^2}{B_1^2+(\beta\mathcal{G}a)^2} \times\left[\ln\left(\frac{4\sqrt{B_1^2+(\beta\mathcal{G}a)^2}}{B_1}\right)+\frac{1}{2}\right]\right\}. \tag{A13}$$

In the approximation $a \approx A$, one obtains Eq. (17).

[1] J. A. Sidles, J. L. Garbini, K. J. Bruland, D. Rugar, O. Züger, S. Hoen, and C. S. Yannoni, Rev. Mod. Phys. **67**, 249 (1995).

[2] N. Nestle, A. Schaff, and W. S. Veeman, Prog. Nucl. Magn. Reson. Spectrosc. **38**, 1 (2001).

[3] A. Suter, Prog. Nucl. Magn. Reson. Spectrosc. **45**, 239 (2004).

[4] B. C. Stipe, H. J. Mamin, C. S. Yannoni, T. D. Stowe, T. W. Kenny, and D. Rugar, Phys. Rev. Lett. **87**, 277602 (2001).

[5] D. Rugar, R. Budakian, H. J. Mamin, and B. W. Chui, Nature (London) **430**, 329 (2004).

[6] G. P. Berman, D. I. Kamenev, and V. I. Tsifrinovich, Phys. Rev. A **66**, 023405 (2002).

[7] G. P. Berman, F. Borgonovi, and V. I. Tsifrinovich, Quantum Inf. Comput. **4**, 102 (2004).

[8] N. N. Bogolubov and Y. A. Mitropolsky, *Asymptotic Methods in the Theory of Non-Linear Oscillations* (translated from Russian), (Hindustan Pub. Corp., Delhi, 1961).